Additive Manufacturing 28 (2019) 456–463

Contents lists available at ScienceDirect

Additive Manufacturing

journal homepage: www.elsevier.com/locate/addma

In situ monitoring of material jetting additive manufacturing process via impedance based measurements

Logan D. Sturm[a], Mohammed I. Albakri[b], Pablo A. Tarazaga[b], Christopher B. Williams[a,*]

[a] Design, Research, and Education for Additive Manufacturing Systems Laboratory, Department of Mechanical Engineering, Virginia Tech, Blacksburg VA, 24061, United States

[b] Vibrations, Adaptive Structures, and Testing Laboratory, Department of Mechanical Engineering, Virginia Tech, Blacksburg VA, 24061, United States

ARTICLE INFO

Keywords:
Additive manufacturing
Nondestructive testing
In-situ monitoring
Material jetting
Impedance-based monitoring
Photopolymer systems

ABSTRACT

In this paper, the authors explore the use of impedance-based monitoring techniques for in-situ detection of additive manufacturing build defects. By physically coupling a piezoceramic (PZT) sensor to the part being fabricated, the measured electrical impedance of the PZT can be directly linked to the mechanical impedance of the part. It is hypothesized that one can detect build defects in geometry or material properties in-situ by comparing the signatures collected during printing of parts with that of a defect-free control sample. In this paper, the authors explore the layer-to-layer sensitivity for both PZT sensors embedded into printed parts and for a fixture-based PZT sensor. For this work, this concept is evaluated in context of material jetting. A set of control samples is created and used to establish a baseline signature. (e.g., internal voids) are fabricated and their layer-to-layer signatures are compared to a control sample. Using this technique, the authors demonstrate an ability to track print progress and detect defects as they occur. For embedded sensors the defects were detectable at 2.28% of the part volume (95.6 mm^3) and by fixture-based sensors when it affected 1.38% of the part volume.

1. Introduction

The maturation and growing adoption of additive manufacturing (AM) as a means for making end-use products has led to an increased need for part traceability and process monitoring [1]. Unlike prototypes or fixtures, end-use products must often meet rigorous performance standards and be certified before they can be put into use. In particular, the aerospace industry has begun to implement AM technologies for fabricating high value, low volume parts. Some examples of AM parts being produced and tested include direct printed metals (e.g., Rolls Royce Trent-XWB bearing [2]) and polymers (e.g., FAA-approved ULTEM 9085 aircraft air duct created by Stratasys and Orbis [3]). While traditional quality control focuses on post-process inspection of parts, in situ monitoring is desirable in AM for two reasons: to detect defects before they become internal to the part, and to save cost by detecting defects before the entire build has been completed.

1.1. In situ monitoring of AM

As AM has become more mature, there has been an increasing amount of research into in situ monitoring techniques for all AM processes. In particular, there has been a strong focus on the performance of metal AM processes such as powder bed fusion (PBF) and directed energy deposition (DED). In situ monitoring approaches fall into three categories: surface (monitoring the top layer), volumetric (monitoring through some depth into a part), and indirect (monitoring the machine performance instead of the part). In the first case, the primary focus is with monitoring the formation of a layer either through optical technology or by monitoring the thermal characteristics (e.g. meltpool temperature or extrudate temperature). These monitoring techniques are able to identify defects that occur on the surface of the part, such as geometry changes or small voids, but they lack the ability to directly measure the material properties of the part [4]. Volumetric approaches such as acoustic emission testing, ultrasonic testing, impedance-based testing, eddy current testing, or x-ray computed tomography (CT) can detect internal defects below the surface of a part and may be able to detect changes in the material properties of a part. Indirect monitoring may be able to predict that a part will contain a defect, but it is unable to directly detect defects in the part.

One of the most popular approaches for in-situ monitoring in AM systems is surface monitoring using image based sensors. For powder bed fusion (PBF) and directed energy deposition (DED). A variety of research approaches have been presented [5–7] including optical (using high-speed cameras) [8–11], monitoring of the laser [12], and infrared

* Corresponding author.
E-mail address: cbwill@vt.edu (C.B. Williams).

https://doi.org/10.1016/j.addma.2019.05.022
Received 18 February 2019; Received in revised form 17 May 2019; Accepted 21 May 2019
Available online 22 May 2019

[13]. Some optical methods focus on monitoring the entire layer while other in-situ systems focus on monitoring the melt pool or melt plume instream of the entire build area since this allows for increased resolution [14]. Another method is through the use of an illumination laser in combination with a high-speed camera [15]. Similar approaches have been used for fused filament fabrication, with optical monitoring [16] and laser scanning [17]. For stereolithography, interference monitoring has been used to detect curing and monitor geometry [18].

The body of research for material jetting is significantly smaller than that for metal or extrusion based systems. For polymer systems, the use of IR LEDs and detectors to monitor spatial location of droplets has been demonstrated [19]. For liquid metal jetting, a CCD camera and strobing LED have been used to monitor droplet shape for quality assurance purposes [20]. In both cases, these approaches are limited to monitoring single or small numbers of nozzles and are currently not suited for the large jetting arrays used in many commercial systems. These systems also do not monitor the material properties of the process. While optical techniques limit inspection to the surface geometry of the part at each layer, when used in-situ, surface techniques are able to monitor cross-sections of the part throughout the print. In this way, in-situ surface techniques are able to approximate volumetric inspection of the part. The limitation of this approach is that surface inspection is unable to capture any changes that occur below the layer being monitored. Surface monitoring cannot directly detect thermal or other effects that propagate down through many layers.

With machine behavior, the focus is on detecting when the machine is operating outside of normal parameters. In traditional manufacturing processes, like CNC milling, the material properties are fixed and only the geometry and surface finish need to be monitored. In AM both the material properties and the geometry can by affected by the process parameters and toolpath used to fabricate the geometry can affect the internal material properties of the part. Monitoring process parameters can detect potential build failures, but does nothing to directly monitor the material properties of the part [21].

Other approaches exist to monitor the thermal characteristics of the system using thermocouples and pyrometers [7,22,23]. Ultrasonic [24–26] and laser ultrasonic [4] testing has also been investigated as a means for detecting surface defects and they have some capability to detect volumetric properties such as thickness and internal defects. Acoustic emission (AE) testing is another vibration-based approach that detects energy released from irreversible changes that occur on a micro scale in a part when it is loaded (e.g. crack growth) [27,28]. Thermography can detect internal defects close to the surface by monitoring the heating and cooling of an object, as defects cause irregularities compared to the bulk material properties [27]. More exotic methods of in-situ inspection have also been considered, such as neutron diffraction and X-ray backscattering [29]. These methods can detect defects volumetrically, but require expensive radiation sources. Some work outside of direct-metal AM has been conducted using a variety of sensors and integrating their results together. This work has demonstrated the use of data fusion techniques to leverage signals from thermocouples, accelerometers, an IR temperature sensor, and a borescope to monitor and detect build defects in an material extrusion process [30,31].

An ideal monitoring technique for AM would be able to monitor material properties and geometry layer-by-layer. This technique could be used to qualify parts and would be inexpensive and non-invasive. While current monitoring techniques are able to achieve some of these qualities, they are limited in others (e.g. optical layer-by-layer imaging cannot interrogate material properties throughout the part, x-ray CT scanning can volumetrically image a part, but is expensive [32]).

1.2. Impedance-based monitoring

Based on the previous work that has been done on in-situ monitoring, the authors believe that there is still a need for additional in-situ monitoring techniques that are able to directly interrogate both the material properties and the geometry of the entire part as it is being fabricated. One technique that has been used successfully in structural health monitoring (SHM) applications is impedance-based monitoring. This technique utilizes piezoelectric materials, specifically lead zirconate titanate (PZT) wafers, as collocated sensors and actuators to simultaneously excite the structure and measure its response [33,34].The fundamental basis for impedance based SHM is that the presence of damage will alter the mass, stiffness, or dampening characteristics of the structure, which in turn reflects on its measured dynamic response. Impedance based SHM has been shown to be a promising, non-intrusive, cost-effective, and sensitive solution for real-time damage assessment [35].

Ultrasonic testing and acoustic emission testing share some similarities with impedance based monitoring (e.g. all are vibration-based approaches) however, there are several important differences. Acoustic emission occurs when a material undergoes irreversible changes in its internal structure during mechanical loading. This limits detection to dynamic defects (i.e. a defect can only be detected once and if missed, higher loading is need). While AE can detect very small cracks (25 um) it requires a reference signature and is best suited for continuous testing. Ultrasonic testing is able to detect internal defects by propagating waves through a part and monitoring their reflections. This allows for accurate localization of defects within a part; however it also means that the waves need a clear path to be able to travel along. In a complex part like a lattice structure, waves may be unable to reach a location hidden from “line-of-sight” and therefore any defects in that location will be undetectable [36]. Impedance based monitoring is steady state instead of dynamic and monitors the impedance response of the entire part at a given frequency [37,38]. This allows it to repeatedly identify the same defect (unlike AE) and to detect defects that are hidden from “line-of-sight” since they affect the overall response of the part.

In an AM context, each part design has a distinct mass, stiffness, and dampening response that can be detected through impedance-based monitoring. The introduction of a defect into a part will cause a corresponding change in the response. By physically attaching a PZT sensor to a part, it is possible to couple the mechanical response of the system to the electrical response of the sensor. In a manufacturing context, this means that a simple electrical signal can be used to evaluate the mechanical properties of a part without the need for destructive testing. The authors’ previous work has established that piezoceramic sensors can be used as a post process NDE tool to detect defects in fully fabricated AM parts [39]. An initial series of defect free control parts, are fabricated and measured using this technique to establish a baseline response signature. These control parts can be validated as needed with methods such as CT scanning and destructive testing. Once a baseline signature has been established, the signature of each subsequent part is compared to the baseline to determine if a defect has occurred. In post process inspection, this technique detected defects as small as 8 mm^3 in polymer AM parts fabricated by material jetting and material extrusion [39].

The overall goal of this paper is to assess the feasibility of using electromechanical impedance measurements for in-situ non-destructive evaluation of AM parts. For in-situ impedance -based monitoring a similar approach is proposed. After mounting, sensors monitor several control parts at select layers during fabrication. These control parts are validated and a baseline signature is generated for each layer. As new parts are fabricated their signatures are compared to the baseline signature at each monitored layer. If the variation in the part signature exceeds the established variation threshold it indicates the presence of a build defect.

There are three primary goals for this research. The first goal is to assess the feasibility of using impedance-based monitoring in-situ. The second is to compare approaches for mounting the sensors in-situ, specifically by comparing embedded sensors to fixture based sensors.

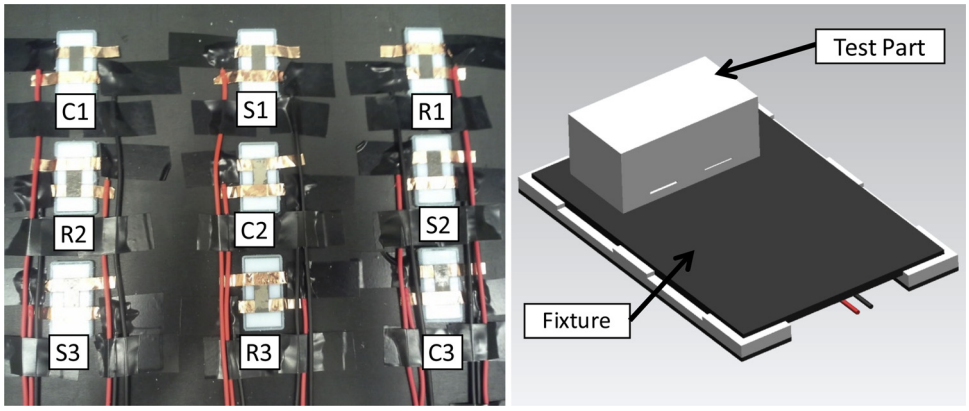

Fig. 1. A) Example of embedded sensor method B) Example of fixture based sensor method.

The third is to determine the size of the defects that are detectable when using impedance based measuring in-situ on plastic AM parts, specifically VeroWhite parts made using material jetting.

2. Experimental methods

2.1. Method overview

The first goal of this study is to evaluate the suitability of using impedance-based monitoring in-situ on an AM system. To investigate this, the authors' designed (i) a test part that a sensor could be embedded into during fabrication, and (ii) a fixture with a mounted sensor on which parts could be fabricated. After embedding the sensor, multiple measurements are taken to ensure that a consistent baseline can be obtained.

The second goal is to compare two methods of in-situ monitoring, embedded sensors and fixture-based sensors. In the first case, the sensor is embedded in a small cavity in the part during fabrication (Fig. 1 A). This method permanently attaches the sensor to the part and requires a separate sensor for each test part. In the second case, a sensor is mounted to a fixture and the parts are directly fabricated on the fixture (Fig. 1B). After fabrication, the part is removed and the fixture is reused. In this way a single sensor (or set of sensors) can be used to measure a large number of parts. To compare these two methods, two identical sets of parts are fabricated: one using the embedded technique and the other using the fixture technique and the sensitivity of both methods are compared.

The final goal is to determine the resolution of defects that in-situ sensing can detect. To accomplish this, a defect with an increasing size is fabricated. During fabrication, measurements are taken at set intervals and compared to the baseline signature. When the deviation from the baseline becomes significant, the layer number is noted and used to calculate the size of the defect based on the model. Since the defect is increasing in size, the first layer that the defect is detected on indicates the size of the smallest detectable defect.

2.2. Material jetting process

Material Jetting (MJ) is an AM process that uses an array of nozzles to selectively deposit material (usually a resin) that is cured by a broad area energy source (e.g. a UV lamp). These systems can offer high resolution (droplet and layer sizes < 100 microns) and are used for fabricating dental and medical models [40]. Material jetting systems also have the ability to fabricate models using multiple materials, which allows for performance testing of composite (hard/soft) designs [41,42]. In the context of this study, material jetting was chosen due to accessibility of the system for embedding sensors and for the ability to selectively change the material/stiffness of a part while maintaining the overall geometry and mass. While material jetting was selected, the monitoring process as used should also be applicable to extrusion systems, and potentially stereolithography systems.

2.3. Materials

All parts were printed using a Stratasys Connex 350 with a resolution of 300 × 600 DPI in the x–y plane with 0.03 mm layers [43]. The material used was VeroWhite [44] (a hard acrylate based photopolymer), and SUP705 support material with a matte finish. VeroWhite was chosen because it is a standard material used for fabricating parts on this system. While the specific results, such as sensitivity, cannot be directly transferred to other materials (e.g. stiffer materials may be more sensitive, softer materials may be less), the general approach and methods should be applicable to different types of materials as demonstrated in the authors' previous work [39]. The piezoelectric material was 0.1905 mm thick lead zirconate titanate (PZT) wafers [45] cut into 20 mm x 8 mm pieces. Cyanoacrylate was used to bond the sensors to the part and the fixture. Copper tape with a conductive adhesive and flux core solder were used to attach electrodes to the PZTs. The fixture consisted of 1/8" acrylic sheet and 1/16" stainless steel cut into a 2" x 3" section and mounted on top of a 3D printed stand.

2.4. Test specimen design

For the embedded sensing, two test parts were designed, (i) a control (Fig. 2A, "A") and (ii) a triangular prism cavity (Fig. 2B, "B"). The triangular cavity feature was chosen so that the defect would start small and grow increasingly larger with each layer. The defect simulates the effect of a void being placed in the model file. Both parts also contained

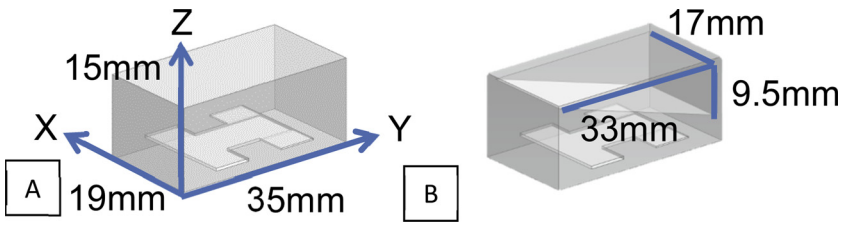

Fig. 2. Test parts A) Control sample "A", B) Triangular prism cavity "B" (lines indicate defect dimensions).

a small cavity at the base for embedding the PZT sensor/actuator. The piezos are embedded after 2.5 mm (layer# 83) of the parts have been printed. The defects begin after 4.5 mm (layer# 151). The thickness of the wall containing the defects is 1 mm. Part "B" has a right triangular cross-section with dimensions shown in Fig. 2B. The total volume of the defect is 2665 mm^3 (26.7% of total volume). Due to the ramp shape, the size of the fabricated defect increases with each layer and the smallest increase in defect size in a layer is 0.027 mm^3 (0.00027% of total volume).

2.4.1. Embedded measurements

Because the defect is enclosed, it will be filled with a supporting material that has similar density, but significantly different stiffness. The mass and geometry of the part remain the same. The defect does simulate how a void in the model file would be fabricated (e.g. through a malicious cyber-attack [46]), and the substitution of model material for support material weakens a part in a similar way that an empty void would.

Three copies of each test part were printed simultaneously, arrayed in a random layout. The print was paused at the completion of the small cavity (2.5 mm, layer# 83) and support material was removed. The sensors were bonded to the parts and allowed to set for one hour. After resuming printing, measurements were taken at the layers shown in Table 1. To avoid any interference in the signal caused by the machine operating, the printer was paused before each measurement and resumed after all parts had been measured (~5 s per part).

2.4.2. Fixture-based measurements

For the fixture-based sensing, a PZT sensor was prepared similarly to the embedded sensors, but was mounted to a steel sheet using cyanoacrylate. Steel was chosen as the fixture material because initial experiments with acrylic demonstrated that the stiffer material transferred vibrations better, resulting in better signatures. After the sensors were mounted to the sheet, the piece was placed on top of a 3D printed fixture aligned to the top left corner of the build area. Parts were printed one at a time and a single measurement was taken at each layer shown in Table 1 without pausing the printer. A total of three control samples and three defective parts were printed on the fixture for a total of six prints. To ensure good transfer of vibration, the standard pedestal of support material was removed for the fixture prints and they were built directly on the fixture surface. The defect starts in layer 151, which is 4.23 mm into the print.

Table 1
Part layers where measurements were taken. For each layer, the volume of model material in each part is shown along with the size of the defect, and the percentage of the printed material that the defect represents.

Part Height		Model Material Volume mm^3		Defect Size
mm	Layer	Control	Defect	%
4.20	140	2793.0	2793.0	0.00%
4.35	145	2892.8	2892.8	0.00%
4.50	150	2992.5	2992.5	0.00%
4.65	155	3092.3	3091.6	0.02%
4.80	160	3192.0	3189.3	0.08%
4.95	165	3291.8	3285.8	0.18%
5.10	170	3391.5	3380.9	0.31%
5.25	175	3491.3	3474.7	0.48%
5.40	180	3591.0	3567.1	0.67%
5.55	185	3690.8	3658.2	0.88%
5.70	190	3790.5	3748.0	1.12%
5.85	195	3890.3	3836.5	1.38%
6.00	200	3990.0	3923.6	1.66%
6.30	210	4189.5	4093.9	2.28%
6.60	220	4389.0	4258.9	2.96%
6.90	230	4588.5	4418.6	3.70%
7.20	240	4788.0	4573.0	4.49%
7.50	250	4987.5	4722.0	5.32%

2.5. Impedance measurements and analysis

The response of the sensor was measured using a Keysight E4990A impedance analyzer over a frequency range of 10–100 kHz. Each embed part was measured (~5 s per measurement) three times at the end of each of the layers shown in Table 1 and the mean of the measurements was used for comparison. The fixture-based parts were measured a single time after the layer while the print was running. To quantify the difference between signatures, the damage metric defined in Eq. (1) was used:

$$RMSD = \sqrt{\sum \frac{(Z_D - Z_{BL})^2}{Z_{BL}^2}} \quad (1)$$

Where Z_D is the impedance at a given frequency of the part being measured and Z_{BL} is the impedance at a given frequency of the baseline (established by averaging together the control samples). This damage metric is explained more in detail in the authors' previous work [39]. After establishing a baseline signature and variance with the control samples new specimens are compared to the baseline and if the damage metric is greater than the sample variance it indicates the presence of a defect.

3. Results

3.1. Embedded piezo repeatability

Fig. 3 shows an example of an impedance signature taken at (layer 150#, embedded part A1). As shown in Fig. 3 multiple measurements of a single part at a set layer had very little deviation. The small variations that do occur can be attributed to normal noise experienced by the analyzer when performing impedance measurements. This lack of deviation shows that there is little to no machine interference or sources of random error occurring in the measurements, outside of what is normally expected from the monitoring equipment.

3.2. Embedded piezos

Fig. 4a. provides a visualization of the damage metric (Eq. (1)) calculated from comparing control to defect specimens each part at each layer. The y-axis indicates the sample and the x-axis indicates the layer number. Thus each cell in the array represents the comparison of a signature, like the one shown in Fig. 3, to the baseline signature using the RMSD (Eq. (1)) damage metric. In this representation, dark purple (as shown on the baseline row) indicates little to no difference from the baseline signature at that layer. Brighter colors indicate increasingly large deviations from the baseline signature. The difference is deemed significant when the damage metric indicates a greater change in the defective parts than the variance in the control parts.

The red line indicates the layer at which the defect starts to be fabricated (layer# 151) and the red oval indicates the point where the damage metric reports a significant change (i.e. the RMSD is greater than that of the controls). Using the signature from the embedded piezos, the damage metric was able to detect the triangular prism cavity at layer 210 as shown in Fig. 4a. The defect size when detected is 95.6 mm^3 (2.28% of printed volume) (Table 1). Fig. 4b. shows the signature for the controls, baseline, and defective parts at layer 245.

3.3. Fixture-based piezos

When using the damage metric with the steel fixture, it was able to detect the defect at layer 195 (Fig. 5a) This corresponds to a defect of size 53.8 mm^3 (1.38% of printed volume). Mounting the piezo to a steel fixture results in significantly more distinct peaks (due to the higher

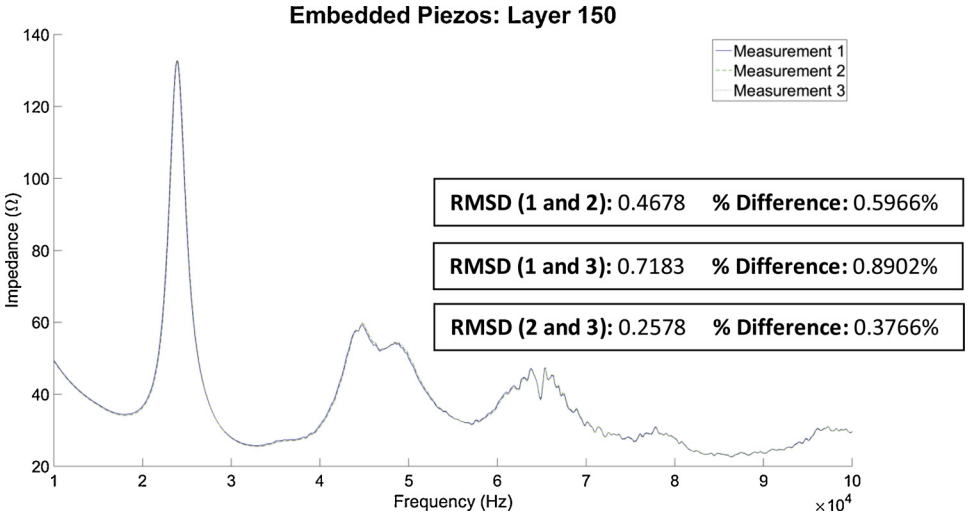

Fig. 3. A comparison of multiple signatures taken at the same layer from the same part using an embedded sensor.

stiffness of the material), the variation between measurements is also significantly reduced. The increased mass of the system significantly reduces the magnitude of the differences. For the best results it is necessary to identify the peaks where the defect is manifested and to compare the curves in those areas, otherwise the noise of small sharp peaks may reduce the sensitivity. By visual comparison of the signatures, it was determined that the defect was manifested in the signature primarily in the following four frequency ranges, 30–33 kHz, 37–40 kHz, 41–44 kHz, and 53–56 kHz. This subset of frequencies was used to calculate the damage metric, which showed a significant difference between the baseline and the defective parts.

4. Discussion

By embedding piezos into printed parts it was possible to detect changes in parts' stiffness introduced by creating cavities containing support material. These defects were detectable as small as 95.6 mm^3 (2.28% of printed volume). Natural variation between each sensor, and differences in how the piezos are mounted, can cause variation in sensor readings. These natural variations introduce noise that effectively reduces the sensitivity of the technique. While smaller print defects might be detectable, the sensor variation results in the resulting signal being undistinguishable from that of the control specimen. Another drawback of the embedding method is that it requires modification of the model design to accommodate the sensor and for the build to be paused to allow the sensor to be embedded.

The fixture-based method addresses these issues by using the same piezo sensor across multiple parts. This eliminates the variation that occurs between sensors and keeps the mounting constant. There still is some variation based on the adhesion of the part to the fixture. This reduction in variation allowed for the defect to be detected 15 layers earlier, at layer 195 instead of layer 210. The use of a fixture adds additional mass to the system, which has the potential to reduce the sensitivity of the system. The signatures showed more peaks in the fixture than for the embedded piezos. This is due to the stiffer steel fixture having more resonance at higher frequencies than the model material. The presences of these peaks present more areas where changes might be detected. The material of the fixture is quite important in transferring the vibrations from the piezo to the part. When using an acrylic fixture, the dampening effect was significant enough to render defects undetectable from baseline variation. A steel fixture has significantly greater stiffness, which allows for better transfer of vibrations from the sensor to the part. Using a steel fixture, it was possible to detect a 53.8 mm^3 defect (1.38% of printed volume). The steel fixture has the ability to detect smaller defects than the embedded piezos. A drawback of the fixture method is the need for the part to be located in the same position each time. Small variation in location will cause changes in the signature. This variation introduces noise that can make the detection of very small defects impossible.

The authors' previous work using impedance-based monitoring as a post processing inspection technique were able to detect internal "voids" as small as 8 mm^3 (0.083% of volume) for the VeroWhite material on the Connex. While the current in-situ work only able to detect defects as small as 53.8 mm^3, the prior work shows that improved resolution should be possible. While this is large compared to the size of droplets (˜100 μm), the nature of material jetting means that small geometric defects will be filled by fluid flow, while large defects will be visible on the surface. Changes to the material properties will be more likely to affect entire layers resulting in much larger affected areas (a single layer of the test part is 19.95 mm^3). Part of for less sensitivity can be attributed to the fact that these techniques are highly dependent on the stiffness of the material being used. The support structure used in Material Jetting has a high amount of dampening, which reduces the sensitivity of the sensors. In post process application, the surrounding support material is removed before the sensors are attached, which may help increase the sensitivity. For the parts with embedded sensors another factor that may reduce the sensitivity is the difficulty of cleaning the embedding location of support material in-situ. Any residual support material would interfere with the attachment of the sensor to the part and could cause variation that would reduce the sensitivity.

The authors believe that the sensitivity of the in-situ measurements could be brought close to that of the post process application with further refinements of the process. It should be noted that these sensitivity results are specific to the material being used, in this study VeroWhite. The use of stiffer materials, such as those found in direct metal AM processes, can significantly improve the ability of the technique to detect small defects. This was shown in the difference between the acrylic and steel fixtures.

Another opportunity for improving sensitivity is in the calculation of the damage metric. While the current technique is capable of detecting differences between signatures, it gives more weight to RMS magnitude differences than changes to the shape of the curve. These shape changes, while potentially small in magnitude, are indicators of significant changes in the response of the part. In parts fabricated on the fixture, the changes in the signatures are happening in a small subset of the frequency range tested. By reducing the range measured, similar to the post-process measurements, and increasing the resolution of the measurements, it should be possible to detect smaller defects without increasing the time needed to acquire the measurements.

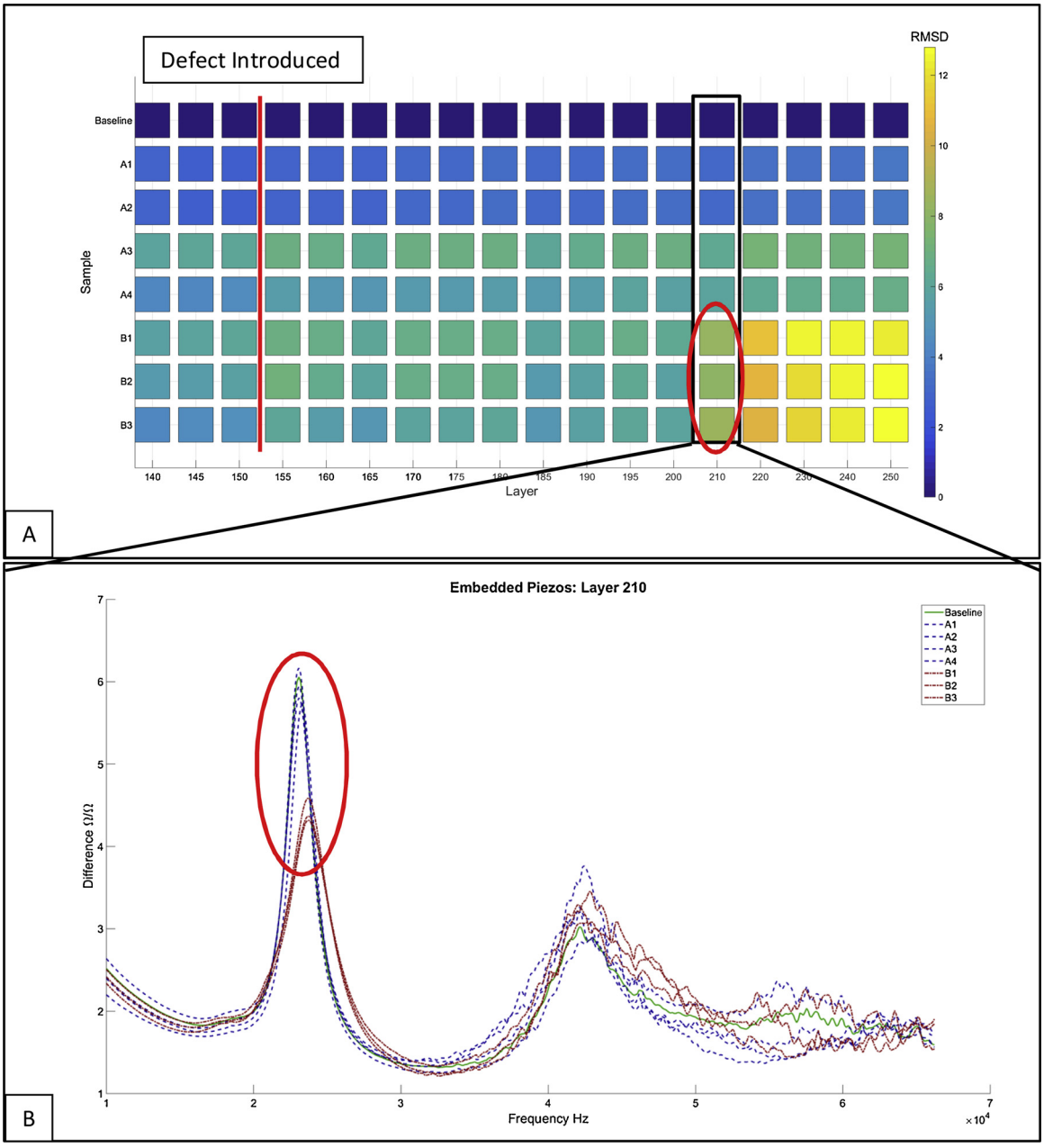

Fig. 4. A) Difference comparison for embedded piezos between baseline, control samples, and defect samples across each layer. The defect is introduced in layer 151 (as indicated by the red line) and detectable in all samples at layer 210 (red oval). The defect size when detected is 95.6 mm^3 (2.28% of printed volume). B) The part signatures at layer 210. The red oval indicates the area where the defect is evident.

5. Conclusions

The layer-by-layer fabrication process of AM systems makes a volumetric evaluation of part quality important. With existing in-situ techniques it can be difficult to directly measure the quality of a part. Because impedance monitoring is linked to the mass, stiffness, and damping of a part, it is able to detect both geometric changes and material property changes volumetrically throughout a part. This ability allows impedance-based monitoring to be used as a side-channel technique (an indirect measurement that can be correlated to the desired properties). The study sucessfully demonstrated the ability of impedance-based techniques to be used as an in-situ monitoring approach for AM. The study demsontrated that both embedded and fixture based approaches were feasible in a Material Jetting system, with the fixture based method being more sensitive to internal defects. Specifically, internal defects could be detected by embedded piezos when they affected 2.28% of the part volume (95.6 mm^3) and by steel fixture-based piezos when they affected 1.38% of the part volume (53.8 mm^3). While this was demonstrated for simple parts the authors' previous work shows that this approach can also be used on complexed geometries [39]. By inspection it was possible to determine the frequency ranges where the defect was manifested in the signature. By narrowing the sampled frequency range it is possible to increase the resolution without increasing the time required. Increasing the sampling resolution should make it possible to increase the resolution of the detection method. The improved performance by increasing the stiffness of the fixture indicates that higher resolution detection should be possible in parts fabricated out of stiffer materials, such as metals.

In future work the authors hope to expand the application of this technic technique to other AM processes, to examine additional types of defects, and to improve the sensitivity by increasing the size/number of the sensor(s), by refining the damage metric to be able to more

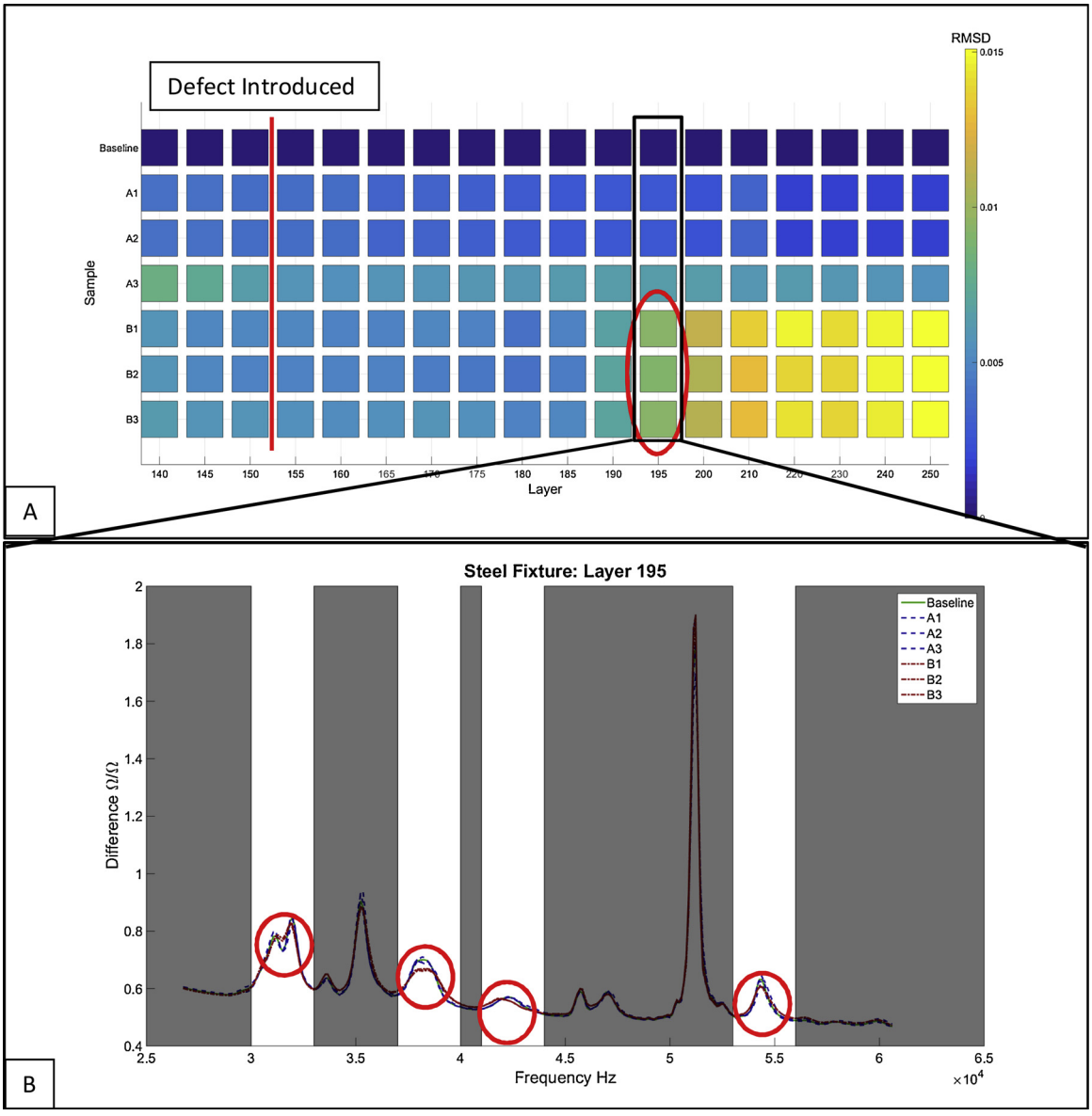

Fig. 5. A) Difference comparison for embedded piezos between baseline, control samples, and defect samples across each layer. The defect is introduced in layer 150 (as indicated by the red line) and detectable in all samples at layer 245 (red oval). The defect size when detected is 53.8 mm^3 (1.38% of printed volume). B) The part signatures at layer 195. The red oval indicates the area where the defect is evident. White areas indicate frequency ranges that were used in analysis.

precisely determine when variation is occurring the signature, and by refining the frequency range being measured.

Conflict of interest

None.

Acknowledgement

This material is based upon work supported by the National Science Foundation under Grant No. CMMI-1436365 and Grant No. CMMI-1635356. Any opinions, findings, and conclusions or recommendations expressed in this material are those of the author(s) and do not necessarily reflect the views of the National Science Foundation.

References

[1] NIST, Measurement Science Roadmap for Metal-based Additive Manufacturing, (2013) http://www.nist.gov/el/isd/upload/NISTAdd_Mfg_Report_FINAL-2.pdf.

[2] D. Howie, High Powered Trent XWB-97, (2015), pp. 12–15 (Accessed January 31, 2017), http://www.rolls-royce.com/media/insights/simon-burr.aspx.

[3] Stratasys, FAA-Approved Air Duct for 'Flying Eye Hospital' Produced in Just Days, (2015) (Accessed January 31, 2017), http://blog.stratasys.com/2015/03/05/3d-printed-air-duct-flying-eye-hospital/.

[4] S.K. Everton, M. Hirsch, P. Stravroulakis, R.K. Leach, A.T. Clare, Review of in-situ process monitoring and in-situ metrology for metal additive manufacturing, Mater. Des. 95 (2016) 431–445, https://doi.org/10.1016/j.matdes.2016.01.099.

[5] G. Tapia, A. Elwany, A review on process monitoring and control in metal-based additive manufacturing, J. Manuf. Sci. Eng. 136 (2014) 60801–60810, https://doi.org/10.1115/1.4028540.

[6] E.W. Reutzel, A.R. Nassar, A survey of sensing and control systems for machine and process monitoring of directed-energy, metal-based additive manufacturing, Rapid Prototyp. J. 21 (2015) 159–167, https://doi.org/10.1108/RPJ-12-2014-0177.

[7] Z.Y. Chua, I.H. Ahn, S.K. Moon, Process monitoring and inspection systems in metal additive manufacturing: status and applications, Int. J. Precis. Eng. Manuf. - Green Technol. 4 (2017) 235–245, https://doi.org/10.1007/s40684-017-0029-7.

[8] S. Berumen, F. Bechmann, S. Lindner, J.-P. Kruth, T. Craeghs, Quality control of laser- and powder bed-based Additive Manufacturing (AM) technologies, Phys. Procedia 5 (2010) 617–622, https://doi.org/10.1016/j.phpro.2010.08.089.

[9] T. Craeghs, S. Clijsters, J.-P. Kruth, F. Bechmann, M.-C. Ebert, Detection of process failures in Layerwise Laser melting with optical process monitoring, PhD 39 (2012) 753–759, https://doi.org/10.1016/j.phpro.2012.10.097.

[10] J. Schwerdtfeger, R.F. Singer, C. Körner, In situ flaw detection by IR-imaging during

electron beam melting, Rapid Prototyp. J. 18 (2012) 259–263, https://doi.org/10.1108/13552541211231572.
[11] R.B. Dinwiddie, R.R. Dehoff, P.D. Lloyd, L.E. Lowe, J.B. Ulrich, Thermographic in-situ process monitoring of the electron-beam melting technology used in additive manufacturing, Proc. SPIE. 8705 (2013), https://doi.org/10.1117/12.2018412 87050K-87050K–9.
[12] A.G. Demir, C. De Giorgi, B. Previtali, Design and implementation of a multi-sensor coaxial monitoring system with correction strategies for selective laser melting of a maraging steel, J. Manuf. Sci. Eng. 140 (2017) 1–14, https://doi.org/10.1115/1.4038568.
[13] M. Grasso, A.G. Demir, B. Previtali, B.M. Colosimo, In situ monitoring of selective laser melting of zinc powder via infrared imaging of the process plume, Robot. Comput. Manuf. 49 (2018) 229–239, https://doi.org/10.1016/j.rcim.2017.07.001.
[14] M. Khanzadeh, S. Chowdhury, M.A. Tschopp, H.R. Doude, M. Marufuzzaman, L. Bian, In-situ monitoring of melt pool images for porosity prediction in directed energy deposition processes, IISE Trans. 0 (2018) 1–19, https://doi.org/10.1080/24725854.2017.1417656.
[15] P. Lott, H. Schleifenbaum, W. Meiners, K. Wissenbach, C. Hinke, J. Bültmann, J. Bültmannc, Design of an optical system for the in situ process monitoring of selective laser melting (SLM), Phys. Procedia 12 (2011) 683–690, https://doi.org/10.1016/j.phpro.2011.03.085.
[16] S. Nuchitprasitchai, M. Roggemann, J.M. Pearce, Factors effecting real-time optical monitoring of fused filament 3D printing, Prog. Addit. Manuf. 2 (2017) 133–149, https://doi.org/10.1007/s40964-017-0027-x.
[17] M. Faes, F. Vogeler, K. Coppens, H. Valkenaers, E. Ferraris, W. Abbeloos, T. Goedeme, Process monitoring of extrusion based 3D printing via laser scanning, Proc. PMI 2014 Conf. (2014), https://doi.org/10.13140/2.1.5175.0081.
[18] X. Zhao, D.W. Rosen, Real-time interferometric monitoring and measuring of photopolymerization based stereolithographic additive manufacturing process: sensor model and algorithm, Meas. Sci. Technol. 28 (2017), https://doi.org/10.1088/0957-0233/28/1/015001.
[19] A. Wang, T. Wang, C. Zhou, W. Xu, LuBan: Low-cost and in-situ droplet micro-sensing for inkjet 3D printing quality assurance, Proc. 15th ACM Conf. Embed. Netw. Sens. Syst. 27 (1-27) (2017) 14, https://doi.org/10.1145/3131672.3131686.
[20] T. Wang, T.H. Kwok, C. Zhou, S. Vader, In-situ droplet inspection and closed-loop control system using machine learning for liquid metal jet printing, J. Manuf. Syst. 47 (2018) 83–92, https://doi.org/10.1016/j.jmsy.2018.04.003.
[21] S.B. Moore, J. Gatlin, S. Belikovetsky, M. Yampolskiy, W.E. King, Y. Elovici, Power Consumption-based Detection of Sabotage Attacks in Additive Manufacturing, (2017), pp. 1–19 http://arxiv.org/abs/1709.01822.
[22] T. Furumoto, T. Ueda, M.R. Alkahari, A. Hosokawa, Investigation of laser consolidation process for metal powder by two-color pyrometer and high-speed video camera, CIRP Ann. Manuf. Technol. 62 (2013) 223–226, https://doi.org/10.1016/j.cirp.2013.03.032.
[23] T. Furumoto, T. Ueda, N. Kobayashi, A. Yassin, A. Hosokawa, S. Abe, Study on laser consolidation of metal powder with Yb:fiber laser—evaluation of line consolidation structure, J. Mater. Process. Technol. 209 (2009) 5973–5980, https://doi.org/10.1016/j.jmatprotec.2009.07.017.
[24] H. Rieder, A. Dillhöfer, M. Spies, J. Bamberg, T. Hess, M.S. Bamberg, H. Rieder, A. Dillhöfer, M. Spies, J. Bamberg, T. Hess, Ultrasonic online monitoring of additive manufacturing processes based on selective laser melting, AIP Conf. Proc. 1650 (2015) 184–191, https://doi.org/10.1063/1.4914609.
[25] H. Rieder, M. Spies, J. Bamberg, B. Henkel, On- and offline ultrasonic characterization of components built by SLM additive manufacturing, AIP Conf. Proc. 1706 (2016), https://doi.org/10.1063/1.4940605.
[26] S. Kenderian, O. Esquivel, K.R. Olson, E.C. Johnson, A general overview of some Nondestructive Evaluation (NDE) techniques for materials characterization, Opt. Mater. Struct. Technol IV (7425) (2009) 742506, , https://doi.org/10.1117/12.826906.
[27] Q.Y. Lu, C.H. Wong, Additive manufacturing process monitoring and control by non-destructive testing techniques: challenges and in-process monitoring, Virtual Phys. Prototyp. 13 (2018) 39–48, https://doi.org/10.1080/17452759.2017.1351201.
[28] S.A. Shevchik, C. Kenel, C. Leinenbach, K. Wasmer, Acoustic emission for in situ quality monitoring in additive manufacturing using spectral convolutional neural networks, Addit. Manuf. 21 (2018) 598–604, https://doi.org/10.1016/j.addma.2017.11.012.
[29] T. Watkins, H. Bilheux, K. An, A. Payzant, R. Dehoff, C. Duty, W. Peter, C. Blue, C. Brice, Neutron Charact. Addit. Manuf. 171 (2013) 23–27 https://ntrs.nasa.gov/archive/nasa/casi.ntrs.nasa.gov/20140005932.pdf.
[30] P.K. Rao, J.(Peter) Liu, D. Roberson, Z.(James) Kong, C. Williams, Online real-time quality monitoring in additive manufacturing processes using heterogeneous sensors, J. Manuf. Sci. Eng. 137 (2015) 61007–61012, https://doi.org/10.1115/1.4029823.
[31] Z. Li, Z. Zhang, J. Shi, D. Wu, Prediction of surface roughness in extrusion-based additive manufacturing with machine learning, Robot. Comput. Manuf. 57 (2019) 488–495, https://doi.org/10.1016/j.rcim.2019.01.004.
[32] A. Thompson, I. Maskery, R.K. Leach, X-ray computed tomography for additive manufacturing: a review, Meas. Sci. Technol. 27 (2016), https://doi.org/10.1088/0957-0233/27/7/072001.
[33] C. Liang, F.P. Sun, C.A. Rogers, Coupled electro-mechanical analysis of adaptive material systems-determination of the actuator power consumption and system energy transfer, J. Intell. Mater. Syst. Struct. 8 (1997) 335–343 10.1177%2F1045389X9700800406.
[34] V. Giurgiutiu, A.N. Zagrai, Characterization of piezoelectric wafer active sensors, J. Intell. Mater. Syst. Struct. 11 (2001) 959–976, https://doi.org/10.1106/A1HU-23JD-M5AU-ENGW.
[35] G. Park, H. Sohn, C.R. Farrar, D.J. Inman, Overview of piezoelectric impedance-based health monitoring and path forward, Shock Vib. Dig. 35 (2003) 451–463, https://doi.org/10.1177/05831024030356001.
[36] Z. Bai, S. Chen, L. Jia, Z. Zeng, Phased array ultrasonic signal compressive detection in low-pressure turbine disc, NDT E Int. 89 (2017) 1–13, https://doi.org/10.1016/j.ndteint.2017.03.002.
[37] D.M. Peairs, P.A. Tarazaga, D.J. Inman, Frequency range selection for impedance-based structural health monitoring, J. Vib. Acoust. 129 (2007) 701, https://doi.org/10.1115/1.2775506.
[38] J.P. Nokes, G.L. Cloud, The application of interferometric techniques to the non-destructive inspection of fiber-reinforced materials, Exp. Mech. 33 (1993) 314–319, https://doi.org/10.1007/BF02322147.
[39] M.I. Albakri, L.D. Sturm, C.B. Williams, P.A. Tarazaga, Impedance-based non-destructive evaluation of additively manufactured parts, Rapid Prototyp. J. 23 (2017) 589–601, https://doi.org/10.1108/RPJ-03-2016-0046.
[40] M.I. Mohammed, B. Cadd, G. Peart, I. Gibson, Augmented patient-specific facial prosthesis production using medical imaging modelling and 3D printing technologies for improved patient outcomes, Virtual Phys. Prototyp. 13 (2018) 164–176, https://doi.org/10.1080/17452759.2018.1446122.
[41] V. Dikshit, A.P. Nagalingam, Y.L. Yap, S.L. Sing, W.Y. Yeong, J. Wei, Crack monitoring and failure investigation on inkjet printed sandwich structures under quasi-static indentation test, Mater. Des. 137 (2018) 140–151, https://doi.org/10.1016/j.matdes.2017.10.014.
[42] V. Dikshit, A.P. Nagalingam, Y.L. Yap, S.L. Sing, W.Y. Yeong, J. Wei, Investigation of quasi-static indentation response of inkjet printed sandwich structures under variousindenter geometries, Materials (Basel) 10 (2017), https://doi.org/10.3390/ma10030290.
[43] Stratasys Ltd, Objet350 and Objet500 Connex3 Spec Sheet, (2017) http://usglobalimages.stratasys.com/Main/Files/Machine_Spec_Sheets/PSS_PJ_Connex3.pdf?v=635836085717699464.
[44] Stratasys Ltd, Polyjet Materials Data Sheet, (2015), p. 3 global72.stratasys.com/~/media/Main/Files/Material_Spec_Sheets/MSS_PJ_PJMaterialsDataSheet.ashx.
[45] P.S. Inc., PIEZOELECTRIC & MATERIAL PROPERTIES OF PSI-5A4E SINGLE SHEETS, (2011), p. 26 http://www.piezo.com/catalog8.pdffiles/Cat8.26.pdf.
[46] L.D. Sturm, C.B. Williams, J.A. Camelio, J. White, R. Parker, Cyber-physical vulnerabilities in additive manufacturing systems: a case study attack on the.STL file with human subjects, J. Manuf. Syst. 44 (2017) 154–164, https://doi.org/10.1016/j.jmsy.2017.05.007.